

**CORE FORMATION WITH IMPLICATIONS TO THE MARTIAN DICHOTOMY: THERMO-CHEMICAL CONVECTION IN A SPHERICAL SHELL.** K. Stemmer<sup>1</sup> and D. Breuer<sup>1</sup>, <sup>1</sup>Institute of Planetary Research, German Aerospace Center (DLR), Rutherfordstr. 2, 12489 Berlin, Germany (Kai.Stemmer@dlr.de).

**Introduction:** A fundamental problem in the evolution of Mars is the timing and the origin of the crustal dichotomy. The southern highlands and northern lowlands of Mars differ markedly in average elevation [1] and crustal thickness [2,3]. Although it is generally accepted that this crustal dichotomy is one of oldest features on Mars, the exact timing of the dichotomy formation, which has implications for the formation mechanism, is strongly debated. Estimates of the dichotomy formation age range between the Late Noachian/Early Hesperian (before  $\sim 3.7$  Ga) [4] and as early as the first 50 Ma after the solar system formation [5]. The origin of the crustal dichotomy has variously been related to external [6,7] and internal processes [8], but none of the proposed formation mechanisms has been fully convincing in part due to the uncertainty in the timing of the dichotomy formation. For the external processes, one impact [6] or several large impacts [7] have been suggested as an explanation of the crustal dichotomy. For an endogenic origin of the dichotomy, three different mechanisms have been proposed that are associated with 1) the instability of a chemically layered magma ocean [9,10] 2) an episode of degree-one mantle convection [11,12] and 3) an early phase of plate tectonics [13].

In the present paper, we suggest that the crustal dichotomy is even formed (or initiated) earlier than it is assumed in the previous models: simultaneously or shortly after core formation. Recent studies on short-lived radio-nuclides (e.g., <sup>182</sup>Hf) indicate that core formation occurred during the first 13 Ma after accretion [e.g. 14]. Estimates of the time scale of the core formation process suggest that for rapid separation both the silicate and the iron need to be fluid at least in the upper part of the planet [e.g. 15]. In such a scenario, iron accumulates at the base of a magma ocean and sinks further to the colder centre of the planet by Rayleigh-Taylor instability. The wavelength of the instability depends strongly on the viscosity structure and the thickness of the fluid iron layer. For a dense fluid iron layer with a low viscosity situated on top of a less dense silicate/iron mantle with a high viscosity, a long wavelength instability can be expected [16] resulting in a degree-one downwelling of the iron and upwelling of the central silicate part. Such a large scale convection flow has also implications on the subsequent mantle flow after core formation and on the crustal formation.

We present a fully spherical model of thermo-chemical convection with a temperature- and pressure-

dependent viscosity to study the process of core formation and the onset of mantle convection.

**The Mathematical Model:** We consider thermo-chemical convection of a Boussinesq fluid at infinite Prandtl number heated from below. The velocity boundary conditions at the top and bottom surfaces of the spherical shell are given by impermeable and shear stress-free conditions with a fixed temperature at the top and isolating boundary conditions at the inner radius of the spherical shell. The set of equations is converted to a non-dimensional form by applying appropriate scales for length, time and temperature. As length scale we use the thickness of the sphere, time scale is the thermal diffusion time and temperature is scaled by the temperature difference between hot iron material and the initially cold silicate mantle. The non-dimensional equations of mass, energy and momentum are,

$$\begin{aligned} \nabla \cdot \vec{u} &= 0 \\ \nabla \cdot (\eta(\nabla \vec{u} + \nabla \vec{u}^T)) - \nabla p + (Ra_T T - Ra_C C) \hat{e}_r &= 0 \\ \frac{\partial T}{\partial t} + \vec{u} \nabla T - \nabla^2 T &= 0 \\ \frac{\partial C}{\partial t} + \vec{u} \nabla C - Le^{-1} \nabla^2 T &= 0 \end{aligned} \quad (1)$$

where a conservation equation for the temperature and the composition has to be considered respectively. In this set of equations, T denotes the temperature, C the composition,  $\vec{u}$  the flow velocity vector, p the dynamic pressure, t the time,  $\eta$  the viscosity and  $\hat{e}_r$  the unit vector in radial direction. The two parameters  $Ra_T$  and  $Ra_C$  are the non-dimensional thermal and chemical Rayleigh numbers, which define the ratio of buoyancy forces to resisting forces,

$$Ra_T = \frac{\rho g \alpha_T \Delta T d^3}{\kappa_T \eta_{ref}} \quad Ra_C = \frac{\rho g \alpha_C \Delta C d^3}{\kappa_C \eta_{ref}} \quad (2)$$

where the density  $\rho$ , the acceleration of gravity  $g$ , the coefficient of thermal expansion  $\alpha$  and the thermal diffusivity  $\kappa$  are assumed to be constant throughout the shell. For isoviscous convection the Rayleigh number is a constant, but for temperature- and pressure-dependent viscosity the local Rayleigh number is a function of viscosity and depth and consequently a function of time and position in the shell. Hence, the definition of the given reference Rayleigh number of the convecting system depends on the choice of the reference viscosity  $\eta_{ref}$ . The viscosity depends on temperature and pressure by an approximation to the Arrhenius relation.

$$\eta = \exp(\ln(\Delta\eta_T)(T_{ref} - T) + \ln(\Delta\eta_p)(R_{top} - r - T_{ref})) \quad (3)$$

In this equation  $\Delta\eta_T$  denotes the viscosity contrast induced on temperature over the domain and  $\Delta\eta_p$  the viscosity contrast induced on pressure. The third similarity parameter is the Lewis number  $Le$ ,

$$Le = \frac{\kappa_T}{\kappa_C} \quad (4)$$

which defines the ratio between the thermal diffusivity  $\kappa_T$  and the diffusivity of the chemical component  $\kappa_C$ . Because the chemical diffusivity is significantly lower than the thermal one for a silicate mantle [17], the Lewis number is very large (up to  $Le=10^{12}$ ). This field approach and the numerical resolution limit the Lewis number to  $Le=100$ .

Due to the comparable large chemical diffusivity in the numerical model, one simulation run is temporally limited to short diffusion times ( $t < 0.5$ ). A comparison of different numerical methods [18] shows, that the temporal and spatial structure of the flow of such a dynamical system is almost identical with a simulation run at infinite Lewis number. The resulting density for such a double-diffusive system is given as follows:

$$\rho^* = Le \text{ Ra}_T T - \text{Ra}_C C \quad (5)$$

**The Numerical Model:** Spectral approaches are usually employed for spherical convection models, which do not allow to take into account lateral variations like temperature-dependent viscosity. This numerical model [19] includes a new discretization formulation of the viscous term, tailored to the finite volume method on a collocated grid, to treat convection in a spherical shell with strong temperature dependent viscosity. This approach has been particularly tailored to run efficiently on parallel computers. The spherical shell is topologically divided into six cubes (figure 1). The equations are formulated in primitive variables in a Cartesian frame of reference. Using a pressure weighted interpolation scheme (PWI) in an advanced SIMPLE pressure correction algorithm, attached to a collocated grid, is one of the basic features of the numerical methods of this model. This particular combination enables a stable and smooth solution of the set of equations to handle strong viscosity variations up to eight magnitudes and high Rayleigh numbers up to  $\text{Ra}=10^8$  and avoids the problem of pressure oscillations caused by mode decoupling.

The Crank-Nicolson method is used for the time stepping. A conjugate gradient solver with a SSOR preconditioner is implemented for solving the pressure correction equation in the SIMPLE algorithm. The numerical model is validated by a comparison of diagnostic parameters of steady-state cubic and tetrahedral convection with other published spherical models.

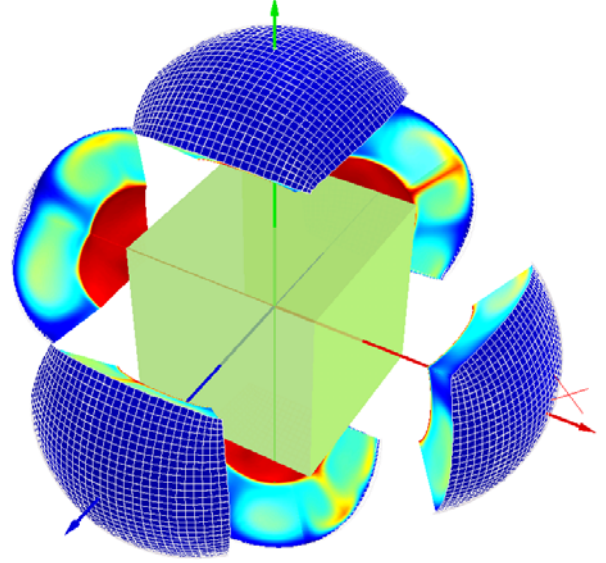


Fig. 1. The exploded smoothed cubed-sphere grid.

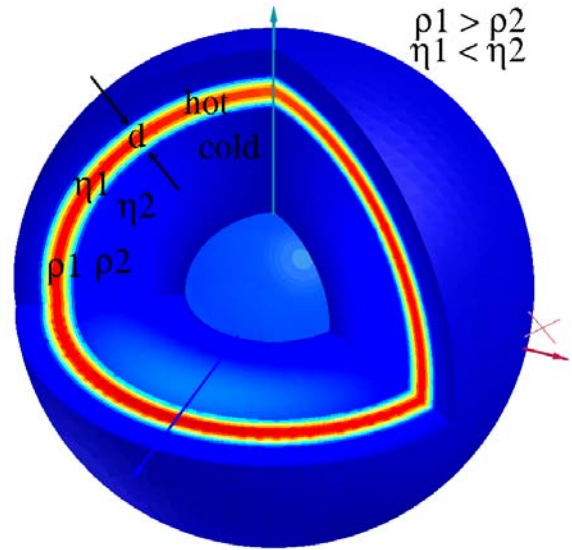
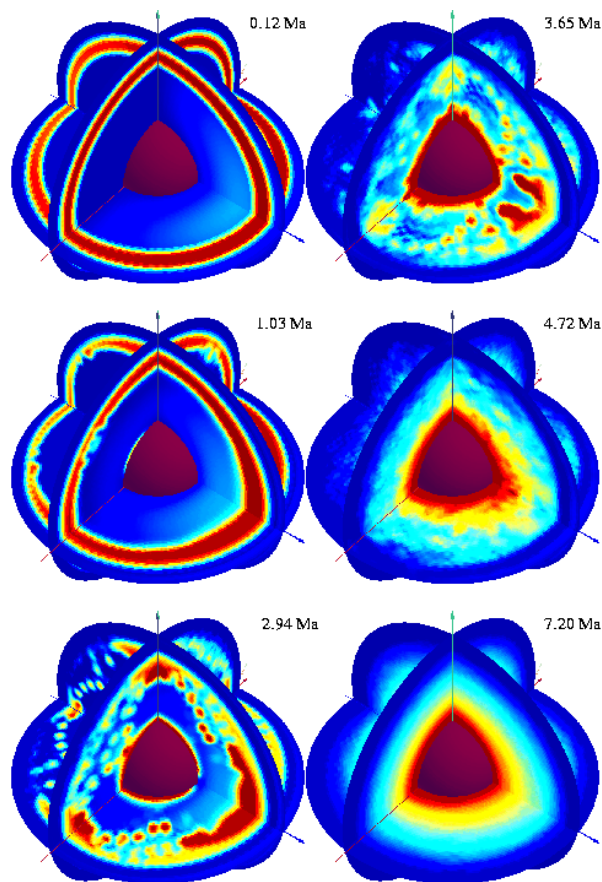


Fig. 2. Initial conditions befor the core formation process starts. The metallic layer (red) is much hotter and more viscous than the surrounding mantle. The viscosity difference  $\Delta\eta_{12}$  and the thickness of the metallic layer  $d$  seems to be of crucial importance for the spatial scales during the core formation process.

**Core Formation:** Meteoritic impacts on the planet causes melting in a near-surface layer. Althow the exact mechanism is not well known, the general agreement is of the very rapid segregation of iron in the melted zone, forming a large metallic layer at the boundary between the melted and solid silicates. Due to the higher density of the metallic layer compared to the cold silicate mantle, an instable layering is existent

(figure 2) in which the metallic layer tends to sink to the planetary interior. We focus on the spatial scales considering this Rayleigh-Taylor instability scenario. Particularly we want to address the requirements which are needed to generate a low-degree instability during core formation. A gravitational instability must occur at long wavelength to explain the crustal dichotomy. It is conceivable that the hemispheric asymmetry at the surface can be explained by a low-degree core formation process which generates an early crust, whereas other authors ascribe the dichotomy to the later processes of one-degree mantle convection considering a weak asthenosphere [12,20] or an endothermic phase transition nearby the core-mantle boundary [21,22].



**Fig. 3.** Snapshots of the dynamics of the metallic material (red) during core formation. Initially the degree-one mode gets the dominant mode (1.03 Ma). On the one hemisphere the layer gets thicker, while on the other one it gets more and more thinner and finally unstable (2.94 Ma). At 3.65 Ma the hemispheres are clearly divided in an downwelling and an upwelling domain and finally (7.20 Ma) a spherical core evolves.

We have accomplished an exemplary simulation of the core formation process. The Rayleigh-Taylor setup includes a temperature- and pressure-dependent rheology with  $\Delta\eta_T=10^3$  and  $\Delta\eta_p=10^1$ , a chemical Rayleigh number of  $Ra_C=10^7$  and thermal Rayleigh number of  $Ra_T=10^5$ . Three-dimensional snapshots (figure 3) of the composition display the temporal evolution of the metallic phase sinking into the planetary interior. A one-degree structure (around 3 Ma) dominates the sinking process superimposed of small scale structures. The spatial scales of the instabilities seems to be strongly dependent on the assumed rheology as well as on the thickness and composition of the metallic layer, which has to be further investigated. We know from two-dimensional simulations of gravitational instability analysis addressing the Moon's hemispheric asymmetry [16], that a thicker layer and a larger viscosity contrast favor a longer wavelength of instability. The depth and thickness, which still increases with depth, of the initial magma ocean is of crucial interest as well as the viscosity contrast between the metallic and silicate material. For a more realistic description of the core formation process, especially in respect to a quantitative analysis of the heat transport towards the core, a variable thermal conductivity and an extended Bousinesq approximation will be considered.

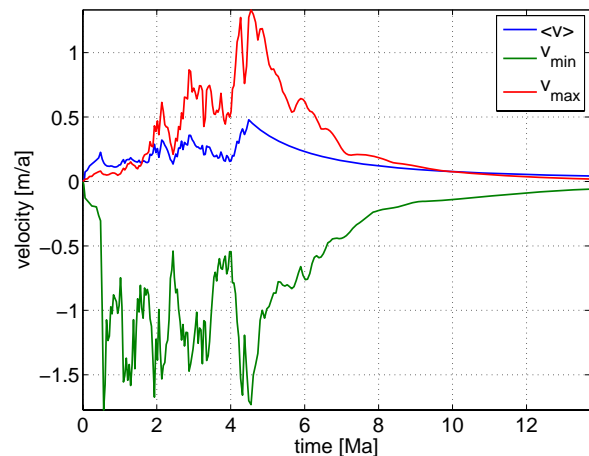


**Fig. 4.** Time evolution of the volume averaged velocity  $\langle v \rangle$  and of the minima/maxima of the radial velocity,  $v_{\min}$  and  $v_{\max}$ . The core formation process is very rapid happening within about 8 Ma for Mars.

The time scale of core formation process is as much important for the heat budget of the planet as the spatial scales of the core formation process. As first approximation the sinking rates of these diapir is estimated by using a Stokes like law [23]. As the underlying silicates are cold, these diapir takes times of the order of one billion years to reach the Martian center,

which would be much too long, as we know from geochemical data of the Earth. Assuming that core formation by negative diapirism is the only core forming process, the downwelling velocity for Mars is derived by [14] with 0.26 m/a, while the whole process happens within 13 Ma. Our simulation confirms that the core formation process can be assumed as rapid as it is derived by [14] (figure 4). While peak velocities are about 1.7 m/a, the volume averaged velocity is about 0.3 m/a and the sinking process of the metallic material is even finished after 8 Ma.

**Onset of Mantle Convection:** If a metallic diapir does cross the cold proto-mantle rather very rapidly and keeps a large temperature due to the gravitational release, a large heat flux is provided as the base of the cold mantle as soon as the core starts forming. On the one hand the time scale of the onset of convection is important to estimate the heat removal from the center of the growing planet, on the other hand the spatial scales of the onset of convection strongly influence the heat budget of the mantle. Assuming a degree-one mantle convection pattern, the surface dichotomy can be explained as a direct consequence of the interior dynamics. Partial melting and thus volcanism is then presumably concentrated on the upwelling hemisphere. The core formation process can be seen as the initial condition triggering the mantle convection and will strongly effect the spatial scales of the flow, at least in the early evolution after mantle convection starts. From our simulations we find that mantle convection would immediately start after the core formation process, which is contrary discussed by [24]. The influence of the core formation process on the onset of mantle convection will be further investigated with this spherical numerical model.

**Summary:** We have investigated the idea that the Martian dichotomy originates from a one-degree core formation process generating an early crust, which is possibly also supported by the following initial mantle convection dynamics. The fully spherical simulation of thermo-chemical convection with temperature- and pressure-dependent rheology considering a Rayleigh-Taylor setup confirm previous studies, that the core formation process is very rapid and happens in the first 50 Ma [5] or even in the first 13 Ma [14]. Of key importance to generate a low-degree pattern of the sinking metallic material is the large viscosity contrast between the metal and the silicate and especially the relatively low viscosity of the metallic material. Furthermore a one-degree core formation process could generate an initially low-degree mantle convection pattern, which could also support a crustal dichotomy. From our findings mantle convection starts immediately after

the low-degree core formation process, which is contrary discussed by [24].

**References:** [1] Smith et al. (1999), *Science*, 284, 1495-1503. [2] Zuber et al. (2000), *Science*, 287, 1788-1793. [3] Neumann et al. (2004), *J. Geophys. Res.*, 109, E08002. [4] McGill and Dimitriou (1990), *J. Geophys. Res.*, 95, 12595-12605. [5] Solomon et al. (2005), *Science*, 307, 1214-1220. [6] Wilhelms and Squyres (1984), *Nature*, 309, 138-140. [7] Frey and Schultz (1988), *Geophys. Res. Lett.*, 15, 229-232. [8] Wise et al. (1979), *J. Geophys. Res.*, 84, 7934-7939. [9] Hess and Parmentier (2001), *32nd Annual Lunar and Planetary Science Conference*. [10] Elkins-Tanton et al. (2003), *Meteoritics & Planetary Science*, 38, 1753-1771. [11] Wise et al. (1979), *J. Geophys. Res.*, 84, 7934-7939. [12] Zhong and Zuber (2001), *Earth Planet. Sci. Lett.*, 189, 75-84. [13] Sleep (1994), *J. Geophys. Res.*, 99, 5639-5655. [14] Kleine et al. (2002), *Nature*, 418, 952-955. [15] Stevenson (1990), *Oxford University Press, New York*, pp. 231-249. [16] Parmentier, Zhong and Zuber (2002), *Earth Planet. Sci. Lett.*, 201, 473-480. [17] Huppert and Turner (1981), *J. Fluid Mech.*, 106, 299-329. [18] Van Keken et al. (1997), *J. Geophys. Res.*, 102, 22477-22495. [19] Stemmer, Harder and Hansen (2006), *Phys. Earth Planet. In.*, 157, 223-249. [20] Roberts and Zhong (2006), *J. Geophys. Res.*, 111, E06013. [21] Harder and Christensen (1996), *Nature*, 380, 507-509. [22] Breuer et al. (1998), *Geophys. Res. Lett.*, 25, 229-232. [23] Honda et al. (1993), *J. Geophys. Res.*, 98, 2075-2089. [24] Choblet and Sotin (2000), *Phys. Earth Planet. Int.*, 119, 321-336